AN EXPERIMENTAL STUDY OF THE EFFECTS OF FINITE WATER DEPTH AND LATERAL CONFINEMENT ON SHIPS WAKE AND DRAG.

Étude expérimentale des effets de hauteur d'eau finie et de confinement latéral sur la résistance à l'avancement et les sillages de navires.

Clément Caplier[1], Germain Rousseaux, Damien Calluaud, Laurent David

Pprime Institute, CNRS, University of Poitiers, ISAE-ENSMA, 86962 Futuroscope Chasseneuil, France.

clement.caplier@univ-poitiers.fr, germain.rousseaux@univ-poitiers.fr, damien.calluaud@univ-poitiers.fr, laurent.david@univ-poitiers.fr

ABSTRACT

Wash waves produced by ships disintegrate river banks and coastal lines. This phenomenon of bank erosion is mainly due to the height of the waves. Various factors govern the forming of these waves and their amplitudes: the geometry of the water channel, the shape and the speed of the boat, etc. These factors play an important role on the waves generation but also on the drag of the ship and so on its fuel consumption. Whether to study the impact of wash waves on the ship's environment or its drag, the analysis of the generated wake is essential. Hence a fine characterization of the wave field is necessary. This study proposes a comparison of wakes generated by two generic ships based on a Wigley hull with block coefficients C_b=0.67 and C_b=0.89 respectively representative of maritime and fluvial ships. The wakes generated in deep water and shallow water configurations have been measured for different Froude numbers with non-intrusive optical stereovision methods, giving access to a detailed and complete definition of the generated wave fields. The drag of the ship hulls has also been measured in deep and shallow water configurations with a hydrodynamic balance. The results permit to study the influence of both hull and water channel geometries on the ship's wake, on the amplitude of the far-field generated waves and on the near-field hydrodynamic response. Moreover, resistance curves are obtained for both configurations and highlight the effect of both hull and water channel geometries on the drag coefficient of the ship.

KEY WORDS

Wash waves, wave field, confinement, ship resistance, drag coefficient

RESUME

Les ondes de batillage déstructurent les berges des fleuves, rivières et du trait de côte. Ce phénomène d'érosion des rives est principalement lié à la hauteur des vagues générées par les navires. Plusieurs facteurs régissent la formation de ces vagues et leurs amplitudes : la géométrie de la voie d'eau, la forme et la vitesse du navire, etc. Ces facteurs jouent un rôle important sur la génération des vagues mais également sur la traînée du navire et donc sur sa consommation en carburant. Que ce soit pour étudier l'impact des ondes de batillage sur l'environnement ou sur la résistance à l'avancement du navire, l'analyse du sillage généré est indispensable. Cette étude propose une comparaison des sillages générés par deux carènes basées sur une carène Wigley, de coefficients de bloc représentatifs des navires maritimes et fluviaux. Les sillages générés dans des configurations de voie d'eau profonde et peu profonde ont été mesurés pour différents nombres de Froude avec une méthode de mesure optique non-intrusive, basée sur un principe de stéréovision, donnant accès à une définition complète et détaillée des champs de vagues générés. La traînée des navires a été mesurée avec une balance hydrodynamique. Les résultats mettent en évidence l'influence de la géométrie de la voie d'eau et du bateau sur les sillages générés, sur les amplitudes des vagues du champ lointain, mais également sur la réponse hydrodynamique dans le champ proche du navire. De plus, les courbes de résistance mettent en avant l'effet de la géométrie de la voie d'eau et du bateau sur le coefficient de traînée du navire.

MOTS-CLEFS

Ondes de batillage, champ de vague, confinement, résistance à l'avancement, coefficient de traînée

[1] Corresponding author

1. INTRODUCTION

Various factors govern the generation and the amplitude of wash waves: the bathymetry of the water channel, the geometry and the speed of the ship, etc. When a ship navigates in a waterway of finite water depth, the effects of confinement result, on the one hand, in a change of the shape of the generated wave field [Ekman, 1906 ; Ekman, 1907 ; Havelock, 1908 ; Inui, 1936 ; Crapper, 1964 ; Fang *et al.*, 2011 ; Carusotto and Rousseaux, 2013]. As the shallow water wake shape highly depends on both the water depth and the ship speed, the non-dimensional height-based Froude number $F_h=U/\sqrt{gh}$ (where $U(m.s^{-1})$ is the ship speed, $g(m.s^{-2})$ the gravity and $h(m)$ the water depth in the waterway), allows to distinguish various regimes [Havelock, 1908 ; Elsasser, 2004]. For F_h<0.60, there are no visible effects of finite water depth and the wave field is similar to the deep water V-shaped Kelvin wake [Kelvin, 1887]. This wake is composed of transverse and diverging waves, respectively perpendicular and oblique with respect to the advancing line of the ship. These two wave systems superimpose on a cusp line which defines the envelop of the wake and forms the typical Kelvin angle α=19.47° with respect to the advancing line. That angle remains constant until a threshold ship speed from which it decreases [Taylor, 1893 ; Baker, 1915 ; Whitham, 1974 ; Rabaud and Moisy, 2013 ; Noblesse *et al.*, 2014 ; Darmon *et al.*, 2014 ; Pethiyagoda *et al.*, 2014]. For 0.60<F_h<1.00 the wake is trans-critical, the angle of the wake increases with the ship speed, as well as the wavelength of the transverse waves. At the particular speed corresponding to F_h=1.00, i.e. $U=\sqrt{gh}$, the wake is critical and the envelop of the wake consist in a perpendicular bow wave in front of the ship (α=90°). In addition, the transverse wave disappear and the wake is only composed of diverging waves. For F_h>1.00 the wake is supercritical and the bow waves folds backwards to the ship with respect to the Froude number as α=arcsin(1/F_h). This behavior is reminiscent of the Mach cone in supersonic aerodynamics.

On the other hand, important hydrodynamic effects appear around the ship, when the waterway is confined both vertically and laterally. It has been highlighted by Scott Russell [1898], through his observations and experiments in narrow and shallow waterways during the nineteenth century. The scottish engineer has pointed out the decreasing of the water level around the ship, whose the impact on the river banks is important. Moreover, the ship is subject to squat and there is a risk of touching the ground. Nevertheless, the major effect highlighted by Scott Russell is the apparition of a bow wave in front of the ship, causing an increase of the ship resistance. The effects of both vertical and lateral confinement on the ship resistance are different [Russell, 1840 ; Inui, 1954 ; Inui, 1957]. Indeed, for a given water depth, the effect of the lateral confinement consist in the apparition of a peak in the resistance for a ship speed $U=\sqrt{gh}$, corresponding to a height-based Froude number F_h=1.00. The smaller is the width of the water channel, the higher is the peak of resistance at F_h=1.00. For a given channel width, the decreasing of the water depth results also in the apparition of a peak in the resistance curve but for a different height-based Froude number. Moreover, the smaller is the water depth, the lower is the speed that corresponds to the peak of resistance. In the case of both lateral and vertical confinement, the two effects are in competition and the resulting resistance curve highlights two critical height-based Froude numbers. The theory established by Schijf [1949] leads to the theoretical expressions given in (1). The critical Froude numbers are given as a function of the blockage ratio of the waterway $m=A_b/A_c$ (where A_b is the immersed cross-section of the ship and A_c the cross-section of the waterway), which reflects the importance of both vertical and lateral confinement. These two height-based critical Froude numbers F_{h1} and F_{h2} are plotted against the blockage ratio m on Figure 2.

$$F_{h1}=\left[2\sin\left(\frac{\arcsin(1-m)}{3}\right)\right]^{3/2} \quad , \quad F_{h2}=\left[2\sin\left(\frac{\pi-\arcsin(1-m)}{3}\right)\right]^{3/2} \qquad (1)$$

However, these effects depend on the volume of water that is displaced by the ship. So they will highly depend on its shape and so on its block coefficient C_b. As the navigation in confined water concerns both maritime ships approaching in harbor areas and heavier river ships in waterways, it is necessary to understand the effect of the geometry of the ship on the ship resistance and on the hydrodynamic phenomena appearing in the waterway. For this, the analysis of the generated wake coupled to drag measurements are essential. This work proposes an experimental study of the wakes generated in a towing tank by two hulls representative of maritime and river ships. The wakes have been measured in a deep water and a confined water configuration and for various Froude numbers. The optical measurement method based on a stereo-correlation principle permits a characterization of the whole wake and a fine reconstruction of the generated wave field [Chatellier *et al.*, 2013]. In addition, the drag of the ship has been measured with a dynamometer in both waterway configurations and for both maritime and river hulls. In a first step, the experimental setup of the study will be presented, i.e. the towing tank, the ship hulls and the measurement methods. The deep water and confined water configurations will be stated and finally the wakes and the resistance curves

measured for each configurations will be presented. The effects of the bathymetry of the water channel, the shape and the speed of the ship will be identified et quantified through the analysis of the results.

2. EXPERIMENTAL SET-UP

2.1 Maritime and river ship hulls

The two ship hulls are based on a Wigley hull with a rectangular section [Wigley, 1926]. This hull form is mathematically defined by the parabolic expression given in (2), in which x and y represent respectively the longitudinal and transversal axes of the ship. L represents the length of the hull (L=1.2m) and B its beam (B=0.18m). During the experiments, the draft is D=0.075m. The maritime hull that has been analyzed is a classical Wigley hull noted WH2, where 2 remains the value of the exponent n in (2), of block coefficient C_b=0.67. However, the block coefficients of river ships are around 0.80-0.90. Then another Wigley-based hull of block coefficient C_b=0.89, noted WH8 and for which n=8 in (3), has also been analyzed. This result in a heavier hull shape at the bow and the stern of the ship (Figure 1).

$$y=f(x)=\frac{B}{2}\left[1-\left(\frac{2x}{L}\right)^{n=2}\right], \qquad (2)$$

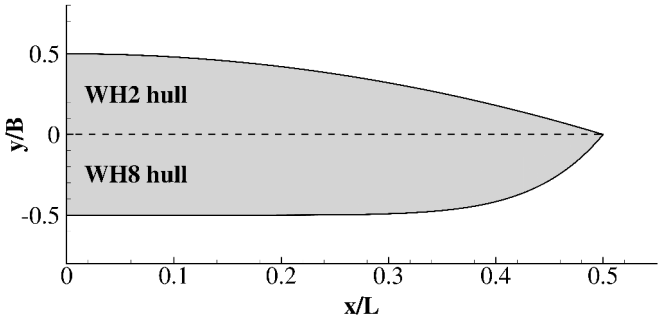

Figure 1: Comparison of the shape of the WH2 maritime hull and the WH8 river hull (only a half of the hull is drawn).

2.2 Towing tank and the waterway configurations

The wakes have been generated in the towing tank of the Pprime Institute. This canal is 20m long and has a rectangular section of width W=1.5m. The water level can be set up to 1.2m and a double bottom can be placed in the canal, to reduce the water level while maintaining the ship hull and the measurement tools fixed. A trolley tows the ship hull along the longitudinal axis of the canal at a speed up to 2.35m.s^{-1}. During the trial, the hull is kept fixed with a vertical mast so that roll, pitch and yaw motions are impossible. Finally, the canal is equipped with windows on its left-side, which allows side-visualizations during the experiments.

The dimensional parameters for the deep water and confined water configurations have been established on the basis of two thresholds. First, a relation established by Zhu *et al.* [2015] gives a threshold on the height-based Froude number, from which the finite water depth has an effect on the undulatory behavior of the generated waves. From observations on analytically calculated shallow water ship wakes, the authors have established that for F_h>0.58 the effects of finite water depth show up. Conversely, the water depth can be considered as infinite for height-based Froude numbers below this threshold. However, this threshold does not reflect the apparition of the hydrodynamic phenomena in the waterway. Thus, an empirical classification established by the International Towing Tank Conference [ITTC, 1987] has been considered. This classification gives limit ratios between the geometric parameters of the waterway and the ship, which correspond to the apparition of the effects of the confinement of the waterway on a hydraulic point of view. These ratios are h/D=4 for the vertical confinement, W/B=4 for the lateral confinement, and $m=A_b/A_c$=0.067 for both.

Considering this, the wakes have been measured for two advancing speeds U=0.8$m.s^{-1}$ and U=1.2$m.s^{-1}$ and two water depths h=0.483m (deep water configuration) and h=0.103m (confined water configuration). This set of parameters, summarized in Table 1, allows to cover a wide range of height-based Froude numbers, while staying under the limit length-based Froude number F_L=0.50 from which the angle starts to

decrease [Taylor, 1893 ; Baker, 1915 ; Whitham, 1974 ; Rabaud and Moisy, 2013 ; Noblesse *et al.*, 2014 ; Darmon *et al.*, 2014 ; Pethiyagoda *et al.*, 2014]. In addition, the wide range of height-based Froude numbers allows to investigate subcritical, trans-critical and supercritical shape wakes. As regards the hydraulic confinement, the width of the canal is the same for each configurations so the lateral confinement will be the same. However, the shallow water configuration is representative of the navigation in confined waters, as both undulatory (F_h>0.58) and hydraulic (h/D<4 and m<0.067) confinement are taken into account.

	deep water		confined water	
$h(m)$	0.483		0.103	
$U(m.s^{-1})$	0.80	1.20	0.80	1.20
F_L	0.23	0.35	0.23	0.35
F_h	0.37	0.55	0.80	1.20
$m=A_b/A_c$	0.088		0.019	
h/D	6.4		1.4	
W/B	8.3			

Table 1: Parameters of the experiments.

Finally, the ship drags have been measured in the deep water configuration for a range of length-based Froude numbers F_L between 0.13 and 0.63, corresponding to height-based Froude numbers F_h between 0.20 and 1.00. As regards the shallow water configuration, the range of length-based Froude numbers is almost the same (between 0.18 and 0.54). However, as the water depth is smaller, the height-based Froude numbers range from 0.60 to 1.85. Hence, this allows to investigate the behavior of the ship resistance around the height-based Froude number F_h=1.00. In addition, the chosen ship speeds cover the theoretical values of the critical height-based Froude numbers F_{h1} and F_{h2} calculated by the Schijf's theory [1949]. The Figure 2 represents the values of F_{h1} and F_{h2} against the blockage ratio of the water way, and the two studied configurations are reminded. In the case of the deep water configuration, the critical height-based Froude numbers corresponding to the blockage ratio m=1/53.7=0.019 are F_{h1}=0.83 and F_{h2}=1.17. For the confined water configuration, the blockage ratio m=1/11.4=0.088 gives the theoretical values F_{h1}=0.65 and F_{h2}=1.37.

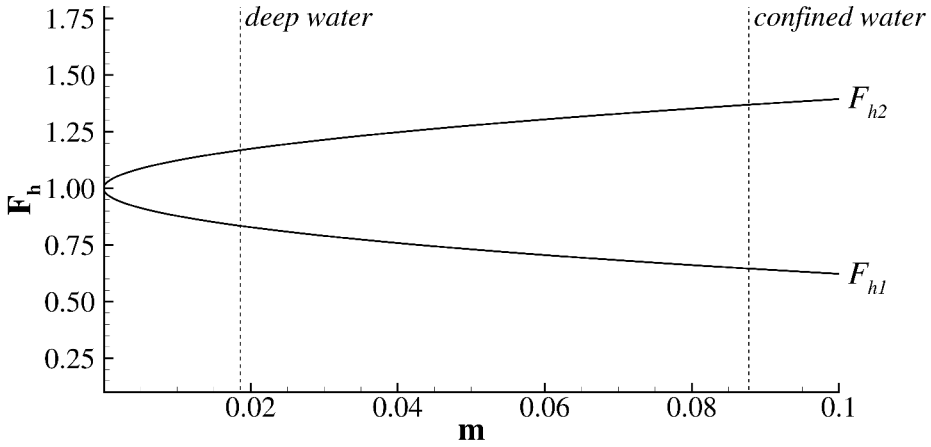

Figure 2: Theoretical values of the critical height-based Froude numbers F_{h1} and F_{h2} given by Schijf's theory [1949].

2.3 Measurement tools

2.3.1 The stereo-correlation method

The wakes have been measured with an optical measurement method based on a stereo-correlation principle [Chatellier *et al.*, 2013]. The method consists in catching the deformation of the free surface at the passage of the ship with two cameras. These two cameras Jai RM-4200CL that deliver a resolution of 2048x2048 pixels and equipped with Nikkor AF 28*mm* 1:2.8 lenses are placed 1.5*m* above the surface of water. They focus on the same zone with an opposite angle of ±15° with respect to the longitudinal axis of the canal, and ±35° with respect to the vertical axis. The common field covered by the cameras forms a rectangle of dimensions 0.75x0.90m^2, corresponding to the half width of the canal. The acquisition of the images is performed with a R&D Vision system, composed by the Hiris software piloted by a synchronization box EG. Then the cameras are synchronized with the start of the ship and the exposure time is set to 10*ms*. The frequency of the acquisition of the images is set at 10 frames per second (fps). The first step of the stereo-

correlation method consist in the calibration of the cameras. For that, a two-dimensional target of points is displaced in the air, along the longitudinal axis of the canal and the camera models are calculated with a dedicated algorithm. Then the canal can be filled up and the surface of water is sowed with floating perlite particles, of size between 1-5*mm*. These particles serve as markers that will follow the free surface deformations at the passage of the ship. Each run is performed three times to check the reproducibility of the measurement. Once the images have been recorded, a correlation algorithm based on the SLIP library [Tremblais and David, 2010] processes the image pairs. The free surface deformation is calculated at each time step with a spatial resolution of 10*mm* and a precision of the water level of 0.1*mm*. Finally, from the three wave fields calculated at each time step, a mean wave field is calculated. Then the whole wake is reconstructed around the ship hull with a dedicated reconstruction program. The result is shown on Figures 3 and 4, in which the black color represents the zones where the computing of the correlation is impossible because of either the absence of particles (chased away by the hull in the middle zone of the waterway), too high wave amplitudes on the banks or wave breaking.

2.3.1 The multicomponent dynamometer and side-visualizations camera

A multicomponent dynamometer Kistler 9272 is placed between the towing mast, which imposes the advancing speed, and the ship hull. It gives access to the three axial components of the force that opposes to the longitudinal motion of the hull, and the momentum around the vertical axis. As the hull is symmetrical and is aligned with the longitudinal axis of the canal, the transverse component of the force and the momentum around the vertical axis are neglectable. Hence only the longitudinal component of the ship resistance is considered for the calculation of the drag coefficients. During the resistance trials, a high-speed camera has been placed on the side of the canal to access to a side-view of the wake generated by the ships, through the windows of the canal. A Photron Fastcam SA1.1 camera, which delivers a resolution of 1024x1024 pixels and equipped with a Sigma 28*mm* F1.8 DG Aspherical Macro lense, performs the acquisition of the images at a frequency of 125*fps* and is synchronized with the start of the ship. Then the images are merged into one single image (Figure 6) with a dedicated program based on the SLIP library [Tremblais and David, 2010].

3. RESULTS

3.1 Ship wakes

The wakes measured in the deep water and confined water configurations are given on Figures 3 and 4, on which the non-dimensional water depth is given as a percentage of the initial water h=0.483*m* or h=0.103*m*. The upper part of each wake corresponds to the river hull WH2 and the bottom part corresponds to the river hull WH8. The wakes measured in the deep water configuration correspond to the classical Kelvin wake pattern, reflecting on the walls of the canal. Whatever the ship speed and its shape, the wake is composed of a transverse and a diverging wave system, and there are no differences as regards the wave-lengths of both wave systems. In addition, a fast geometrical analysis leads to a value of the angle defining the envelop of the wake close to the Kelvin angle α=19.47°. However, the higher block coefficient of the river hull generates a higher bow wave in both cases, and also higher wave amplitudes in the generated wake. A focus on the walls of the canal, for a longitudinal position X/L between 0.5 and 2, highlights these differences. Indeed, for a length-based Froude number F_L=0.23 (top of the figure), the maximum peak-to-trough amplitudes on the wall correspond to 4% of the initial water depth for the maritime hull WH2 and 10% for the river hull WH8. That represents an increase of 150% of the amplitudes of the wash waves reflecting on the walls. For the length-based Froude number F_L=0.35 (bottom of the figure), the difference is less important as the peak-to-trough amplitudes are respectively of 11% and 15% of the initial water depth, for the maritime and river hulls, representing an increase of 40%. In both cases, the waves generated by the river hull are more destructive. Finally, there a no visible effects of the vertical confinement, on both wake's shape and angle, however the lateral confinement implies multiple wave reflections on the wall. Hence, the bow and stern wakes interact and superimpose, leading to the apparition of caustics in the wakes. As regards the wakes generated in the confined water configuration, the effects of both lateral and vertical confinement are present. First, for the length-based Froude number F_L=0.23, corresponding to a height-based Froude number F_h=0.80, the wake is trans-critical on a undulatory point of view: the transverse waves have disappeared and the wake is composed only of transverse waves. As regards the hydraulic confinement, two phenomena highlighted by Scott Russell [1840] have appeared around the ships. The bow wave has straightened up and is perpendicular to the ship, and the lowering of the water level around the hulls extends up to the walls of the canal. In addition, there is a wave-breaking of the first transverse wave generated by

the river hull WH2, which represents a risk for the river banks. For the length-based Froude number F_L=0.35, corresponding to a height-based Froude number F_h=1.20, the wake is supercritical. The wake is now composed only of diverging waves and the bow wave starts to folds backward to the ship [Havelock, 1908 ; Elsaesser, 2006]. This behavior is reminiscent of the Mach cone in supersonic aerodynamics.

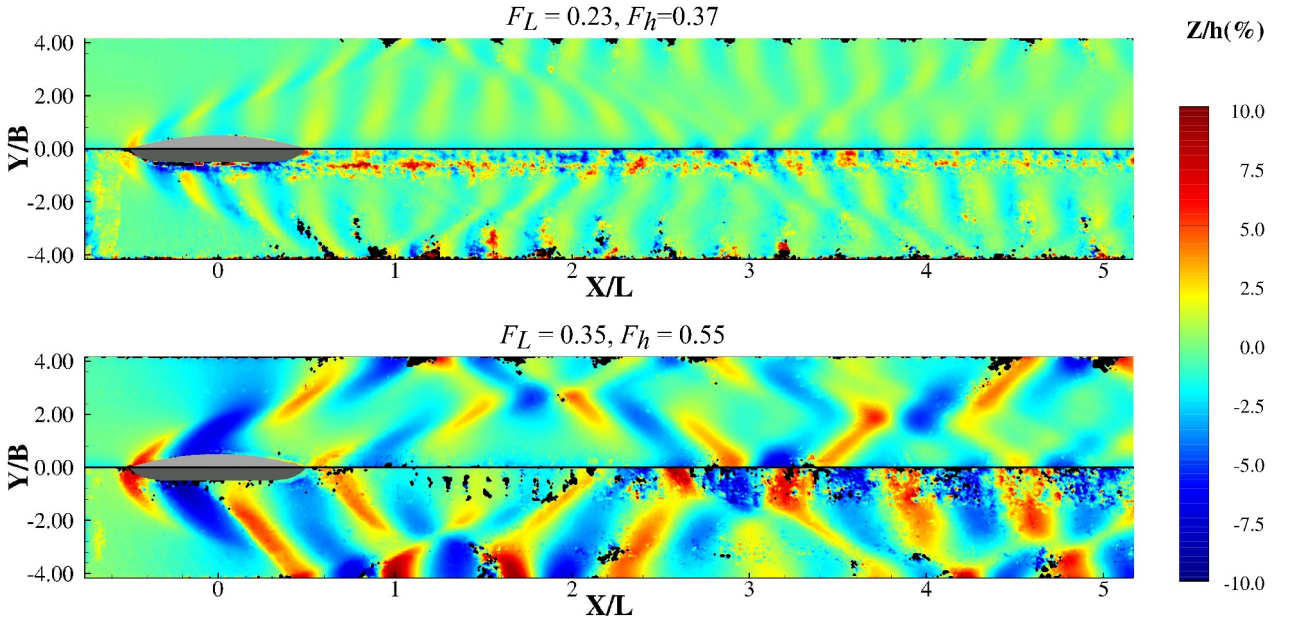

Figure 3: Wakes measured in the deep water configuration. Top: F_L=0.23, F_h=0.37 – Bottom: F_L=0.35, F_h=0.55. The upper part of each wake corresponds to the maritime hull WH2 and the bottom corresponds to the river hull WH8.

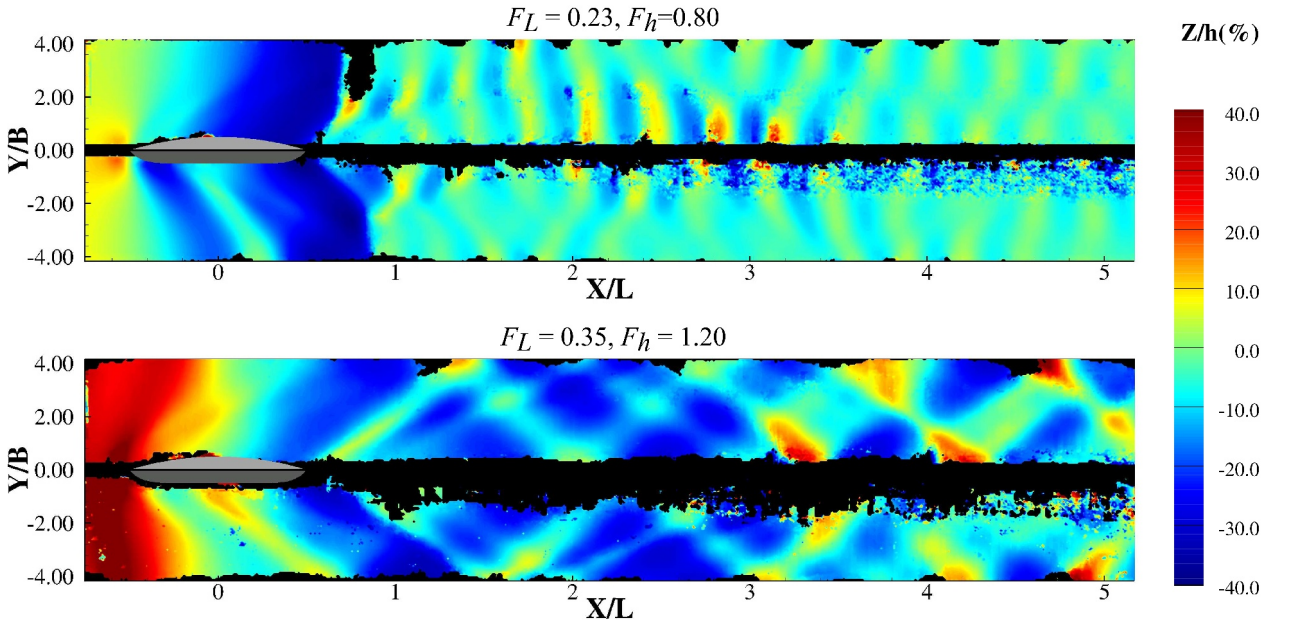

Figure 4: Wakes measured in the confined water configuration. Top: F_L=0.23, F_h=0.80 – Bottom: F_L=0.35, F_h=1.20. The upper part of each wake corresponds to the maritime hull WH2 and the bottom corresponds to the river hull WH8.

3.2 Resistance curves

The Figure 5 represents the drag coefficient C_d of the ship hulls as a function of both length-based and height-based Froude numbers F_L and F_h (respectively the bottom and top x-axes), for the deep water configuration (left) and the confined water configuration (right). The dashed gray lines correspond to the ship speeds for which the wakes have been measured, and the dashed black lines correspond to the theoretical values of the critical height-based Froude numbers given by the Schijf's theory [1949]. The drag coefficient C_d gives a non-dimensional vision of the ship resistance with the ship speed. It is calculated with the formula (3), in which $R(N)$ is the measured force, ρ=1000kg/m^3 the density of the water in the canal and

$U(m.s^{-1})$ the ship speed. The quantity $S(m^2)$ corresponds to the wetted surface area of the ship, calculated with (4), in which $\delta(x)$ defines the contour of the wetted cross-section of the ship hull [Bindel, 1972]. After calculation, the equation (5) is found, giving the relation between the wetted surface area and the geometric parameters of the hulls. In the case of the studied hulls, $S_{WH2}=0.324m^2$ and $S_{WH8}=0.372m^2$.

$$C_d = \frac{2R}{\rho S U^2} , \tag{3}$$

$$S = \int_0^L \delta(x)\,dx = 2\int_0^L \left[y(x)+D\right]dx , \tag{4}$$

$$S = L\left[2D + B C_b\right] , \tag{5}$$

For the deep water configuration, there are oscillations in the drag of the ship for length-based Froude numbers $F_L<0.35$, especially for the maritime hull WH2. These oscillations correspond to the interaction between the bow and stern waves produced by the ship, whose wavelengths depend on its speed. So depending on the ship speed, the constructive or destructive interferences of these two wave systems will generate oscillations in the ship resistance. In addition, for a length-based Froude number $F_L>0.45$, the drag coefficient is constant and starts to decrease for a ship speed corresponding to a height-based Froude number $F_h>F_{h1}>0.83$. Finally, the higher block coefficient of the river hull WH8 implies a higher drag coefficient, as the displaced volume of water is more important. The drag coefficients measured in the confined water configuration have a different behavior with the ship speed and are quantitatively higher than in deep water. The theoretical values of the critical height-based Froude numbers F_{h1} and F_{h2} given by Schijf's theory [1949] correspond to drastic changes in the drag coefficient value. First, there is a sharp increase of the drag coefficient value for a height-based Froude number $F_h>F_{h1}>0.65$. This sharp increase is followed by a plateau on which the drag coefficient is constant and then the drag coefficient decreases suddenly for a height-based Froude number $F_h>F_{h2}>1.37$. The visualizations given on Figure 6 highlight the causes of the fluctuation of the drag coefficient. First, the sharp increase corresponds to the moment when the transverse waves are stuck at the stern of the ship. Then during the plateau the bow wave appears and its amplitude slowly increases. The sudden decrease of the drag coefficient corresponds to the moment when the ship passes over its own bow wave and rides it.

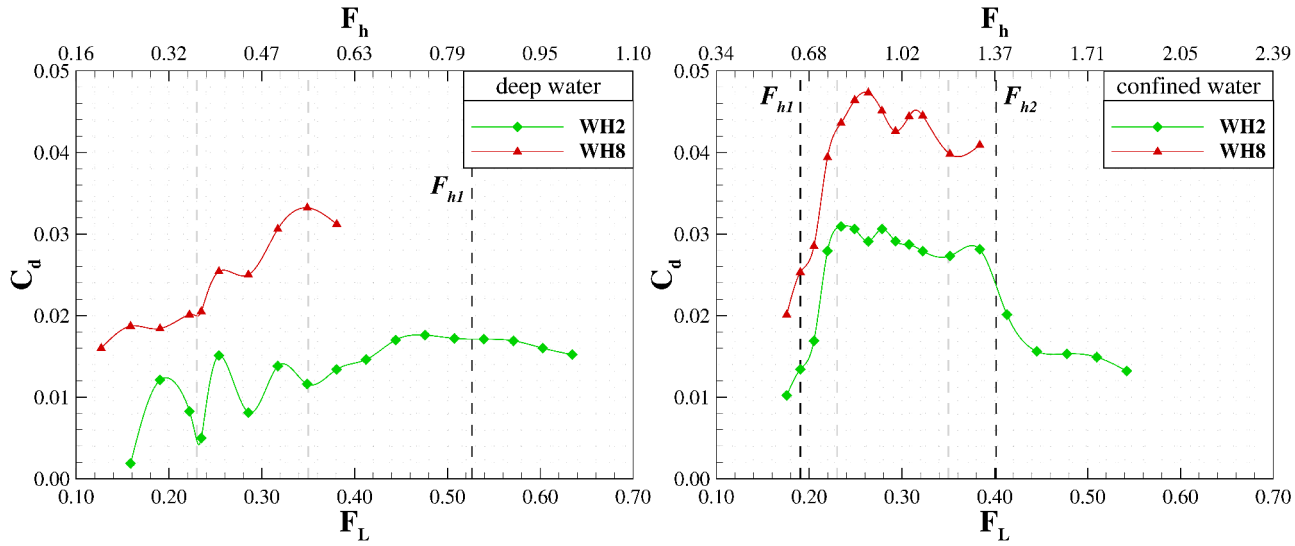

Figure 5: Drag coefficients C_d of the ship hulls as a function of the length-based (bottom x-axis) and height-based (top x-axis) Froude numbers F_L and F_h. The dashed gray lines correspond to the ship speeds for which the wakes have been measured. The dashed black lines correspond to the theoretical values of the critical height-based Froude numbers F_{h1} and F_{h2}. Left: deep water configuration – Right: confined water configuration.

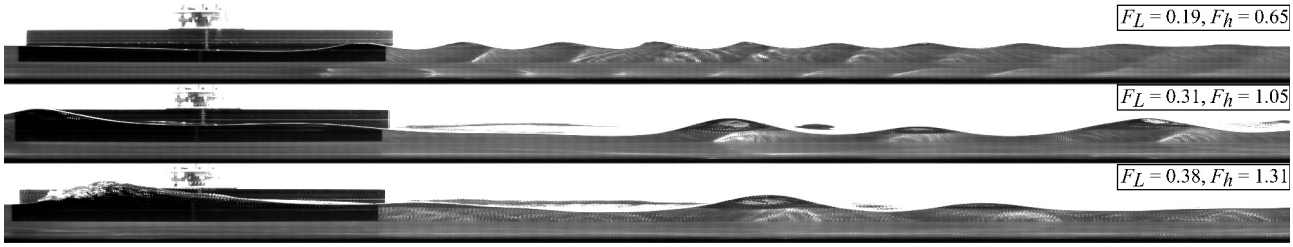

Figure 6: Side view of the wake generated by the maritime hull WH2 in the confined water configuration during the resistance trials, for three different ship speeds (going right to left). Top: F_L =0.19, F_h=0.65 – Middle: F_L =0.31, F_h=1.05 – Bottom: F_L =0.38, F_h=1.31.

5. CONCLUSIONS

The wakes generated by hulls representative of maritime and river ships have been measured in a towing tank. The non-intrusive optical measurement method allowed to identify various wake shapes generated in deep water and confined water configurations, for different ship speeds. The results allowed to highlight the effects of both ship and waterway geometries on the generated wakes. In the deep water configuration, the influence of the ship block coefficient on the amplitude of the wash waves has been highlighted. In the confined water configuration, trans-critical and supercritical wakes have been identified and compared. The effects of the vertical and lateral confinement on both undulatory and hydraulic components of the wakes have been studied. Their influence on the drag of the ship has been emphasized during the resistance trials, combined with side-visualizations of the wakes. However, in a real canal configuration, the current has a strong influence on these parameters. Hence, the measurement of both ship wakes and resistance in a presence of a co- and counter-current of river are necessary.

REFERENCES

Baker G. (1915). – Ship form, resistance and screw propulsion. *D. Van Nostrand Company, London*.

Bindel S. (1972). – Hydrodynamique Navale – tome II (généralités, résistance). *ENSTA Paris Tech*.

Carusotto I., Rousseaux G. (2013). – The Čerenkov effect revisited: from swimming ducks to zero modes in gravitational analogues. *Analogue Gravity Phenomenology, Springer International Publishing, Berlin*, **6**:109-144.

Chatellier L., Jarny S., Gibouin F., David L. (2013). – A parametric PIV/DIC method for the measurement of free surface flows. *Exp. Fluids*, **54(3)**:1-15.

Crapper G.D. (1964). – Surface waves generated by a travelling pressure point. *Proc. R. Soc. Lond. A.*, **282(1391)**:547-558.

Darmon A., Benzaquen M., Raphaël E. (2014). – Kelvin wake pattern at large Froude numbers. *J. Fluid Mech.*, **738**, R3.

Ekman V.W. (1906). – On stationary waves in running water. *Ark. Mat. Astr. Fys.*, **3(2)**.

Ekman V.W. (1907). – On the waves produced by a given distribution of pressure which travels over the surface of water. *Ark. Mat. Astr. Fys.*, **3(11)**.

Elsaesser B., (2004). – The characteristics, propagation and transformation of waves generated by fast marine crafts. *PhD thesis of the Queen's University of Belfast*.

Fang M.C., Yang R.Y., Shugan I.V. (2011). – Kelvin ship wake in the wind waves field and on the finite sea depth. *J. Fluid Mech.*, **27(01)**:71-77.

Havelock T.H. (1908). – The propagation of groups of waves in dispersive media, with application to waves on water produced by a travelling disturbance. *Proc. R. Soc. Lond. A.*, **81(549)**:398-430.

International Towing Tank Conference (1987). – Report of the Resistance and Flow Committee . *Proc. 18th International Towing Tank Conference*, **1**:79-85.

Inui T. (Takao) (1954). – Wave-making resistance in shallow water sea and in restricted water with special reference to its discontinuities . *J. Soc. Naval Arch. of Japan*, **76**:1-10.

Inui T. (Teturô) (1936). – On deformation, wave patterns and resonance phenomenon of water surface due to a moving disturbance. *Proc. Phys.-Math. Soc. Japan, III*, **18**:60-98.

Inui T. (Teturô), Kikuchi Y., Iwata T. (1957). – Shallow water effects on wave-making of ships - A comparison of calculated and measured resistance . *J. Soc. Naval Arch. of Japan*, **100**:35-45.

Kelvin W.T. (Lord) (1887). – On ship waves. *Proc. Inst. Mech. Eng.*, **38(1)**:409.

Noblesse F., He J., Zhu Y., Hong L., Zhang C., Zhu R., Yang C. (2014). – Why can ship wakes appear narrower than Kelvin's angle ?. *Eur. J. Mech. B-Fluids*, **46(0)**:164-171.

Pethiyagoda R., McCue S.W., Moroney T.J. (2014). – What is the apparent angle of a Kelvin ship wave pattern ?. *J. Fluid Mech.*, **738**, R3.

Rabaud M., Moisy F. (2013). – Ship wakes: Kelvin or Mach angle ?. *Phys. Rev. Lett.*, **110(21)**:214.

Schijf J.B. (1949). – Protection of embankments and bed in inland and maritime waters, and in overflow or weirs. *17th Intern. Nav. Cong., Lisbon*, **1**:61-78.

Scott Russell J. (1840). – Mr Scott Russell's researches in hydrodynamics. *Trans. R. Soc. Edinb.*, **14**:47-109.

Taylor D.W. (1893). – Resistance of ships and screw propulsion. *Macmillan and Co, New York.*

Tremblais B., David L. (2010). – Standard Library for Image Processing software. http://sliplib.prd.fr/

Whitham G. B. (1974). – Linear and nonlinear waves. *John Wiley & Sons.*

Wigley W.C.S. (1926). – Ship wave resistance. A comparison of mathematical theory with experimental results. *Trans. of Royal Inst. of Nav. Arch.*, **14**:124-141.

Zhu Y., He J., Zhang C., Wu H., Wan D., Zhu R., Noblesse F. (2015). – Far-field waves created by a monohull ship in shallow water. *Eur. J. Mech. B-Fluids*, **49(0)**:226-234.